Identification of central projections from amylin-activated neurons to the lateral hypothalamus

Potes, C S ; Lutz, Thomas A ; Riediger, Thomas

Abstract: The ability of the pancreatic hormone amylin to inhibit food intake relies on a direct activation of the area postrema (AP). This activation is synaptically transmitted to the nucleus of the solitary tract (NTS), the lateral parabrachial nucleus (LPB), the central amygdaloid nucleus (Ce) and the lateral bed nucleus of stria terminalis (BSTL). Interestingly, neurons of the rostro-dorsal lateral hypothalamic area (dLHA), which are activated during fasting, are inhibited by peripheral amylin, although they lack amylin receptors. Using the retrograde tracer cholera toxin-B (Ctb) we analyzed whether the dLHA receives neuronal projections from amylin-activated brain areas. The anterograde tracer biotinylated dextran-amine (BDA) was used to confirm the projections and to identify further neuronal pathways potentially involved in amylin signaling. We identified dense projections from the amylin activated neurons in the LPB and sparse projections from the NTS to the dLHA. LPB fiber efferents were found in close proximity to dLHA nuclei activated by 24h of fasting. The AP and the Ce showed no projections to the dLHA. Dense efferents were also observed from the LPB to other hypothalamic areas, namely to the ventromedial, dorsomedial, paraventricular and arcuate nuclei. This study provides neuroanatomical evidence that among the amylin activated areas, the LPB provides the strongest input to the dLHA, thus it may mediate the amylin-induced inhibition of the dLHA.

DOI: https://doi.org/10.1016/j.brainres.2010.03.114

Identification of central projections from amylin-activated neurons to the lateral hypothalamus

Catarina Soares Potes, Thomas Alexander Lutz*, Thomas Riediger*

Institute of Veterinary Physiology and Zurich Center for Integrative Human Physiology, University of Zurich, 8057 Zurich Switzerland

*Both senior authors contributed equally to the work

Number of text pages of the whole manuscript: 45

Number of Figures: 7

Number of Tables: 1

Corresponding author:

Thomas Riediger

Institute of Veterinary Physiology, Vetsuisse Faculty University of Zurich

Winterthurerstrasse 260, CH 8057 Zurich, Switzerland

Telephone: +41 44 635 8815

Fax: +41 44 635 8932

Email: triedig@vetphys.uzh.ch

ABSTRACT

The ability of the pancreatic hormone amylin to inhibit food intake relies on a direct activation of the area postrema (AP). This activation is synaptically transmitted to the nucleus of the solitary tract (NTS), the lateral parabrachial nucleus (LPB), the central amygdaloid nucleus (Ce) and the lateral bed nucleus of stria terminalis (BSTL). Interestingly, neurons of the rostro-dorsal lateral hypothalamic area (dLHA), which are activated during fasting, are inhibited by peripheral amylin, although they lack amylin receptors.

Using the retrograde tracer cholera toxin-B we analyzed whether the dLHA receives neuronal projections from amylin-activated brain areas. The anterograde tracer biotinylated dextran-amine was used to confirm the projections and to identify further neuronal pathways potentially involved in amylin signaling. We identified dense projections from the amylin activated neurons in the LPB and sparse projections from the NTS to the dLHA. LPB fiber efferents were found in close proximity to dLHA nuclei activated by 24 hour of fasting. The AP and the Ce showed no projections to the dLHA. Dense efferents were also observed from the LPB to hypothalamic areas, namely to the ventromedial, dorsomedial, paraventricular and arcuate nuclei.

This study provides neuroanatomical evidence that among the amylin activated areas, the LPB provides the strongest input to the dLHA, thus it may mediate the amylin-induced inhibition of dLHA.

SECTION 6 - Regulatory Systems

KEYWORDS: area postrema; rostro-dorsal lateral hypothalamic area; lateral parabrachial nucleus; retrograde tracer; anterograde tracing; neuronal pathways

1 - INTRODUCTION

The maintenance of energy homeostasis is a fundamental requirement for body function. Part of the system controlling food intake and body weight relies on peripheral satiation signals. One of these signals is the peptide hormone amylin, which is co-secreted with insulin from pancreatic beta-cells in response to food intake (Butler et al., 1990; Ogawa et al., 1990) and is considered a physiological satiation signal (Lutz et al., 1995; Lutz, 2005). Chronic amylin administration leads to a sustained reduction in food intake due to a decrease in average meal size and subsequently to a reduction in body weight gain in rats (Lutz et al., 2001). Amylinomimetic agents were shown to reduce eating and decrease body weight in obese human subjects (Aronne et al., 2007; Smith et al., 2007). They also improve blood glucose profiles in diabetic patients (Weyer et al., 2001; Hollander et al., 2004).

The area postrema (AP) of the brainstem, which lacks a functional blood brain barrier, mediates amylin's anorectic action. The important role of the AP has been demonstrated in lesion studies showing that amylin's anorectic effect is blunted in AP lesioned rats (Lutz et al., 1998; Lutz et al., 2001). A direct action of amylin on AP neurons has been confirmed in electrophysiological studies, in which amylin exerted excitatory effects (Riediger et al., 2001). Immunohistochemical studies using the immediate early gene product c-Fos as a marker of neuronal activation showed that peripherally applied amylin not only activates the AP, but also the nucleus of the solitary tract (NTS), the lateral parabrachial nucleus (LPB), the central amygdaloid nucleus (Ce) and the lateral subdivisions of the bed nucleus of the stria terminalis (BSTL) (Rowland et al., 1997; Riediger et al., 2004). These brain structures are part of the central gustatory/enteroceptive systems and are mutually interconnected and linked to the hypothalamus, the main integrative centre for the control of energy balance (Saper, 2002). Since the amylin-induced c-Fos response in the NTS, LPB and Ce was markedly attenuated in AP-lesioned rats, activation of these neurons seems to be synaptically mediated and secondary

to an action of amylin on AP neurons (Rowland and Richmond, 1999; Riediger et al., 2004).

It has been shown that amylin affects hypothalamic centers involved in the control of eating. Amylin and its receptor agonist, salmon calcitonin, decrease the mRNA expression of orexigenic peptides orexin and melanin concentrating hormone (MCH) in the lateral hypothalamic area (LHA) (Barth et al., 2003). In a recent study, we identified a particular group of fasting-activated neurons of unknown neurochemical phenotype that are arranged as a cluster in a defined rostro-dorsal subregion of the LHA, which is termed dLHA in the current work (Riediger et al., 2004). The fasting-induced c-Fos expression in dLHA neurons was attenuated both by refeeding and also by injecting amylin in rats that had no access to food (Riediger et al., 2004). Since amylin administration alone was sufficient to partly reverse the fasting-induced dLHA activation, exogenously applied amylin seems to mimic the ingestion of food, as far as the inhibitory impact on dLHA neurons is concerned. A direct inhibitory influence of amylin on these dLHA neurons is unlikely because the entire LHA is devoid of amylin binding sites (Beaumont et al., 1993; Sexton et al., 1994; van Rossum et al., 1994). Therefore, we hypothesize that the dLHA receives input from amylin-activated neurons of the AP-NTS-LPB-Ce-BSTL axis.

Using retrograde (cholera toxin B, Ctb) and anterograde (biotinylated dextran-amine, BDA) tracing approaches in adult rats, we sought to investigate whether amylin-activated neurons project to the dLHA. To test this we correlated amylin- and fasting-induced c-Fos expression with tracer labeling resulting from local tracer microinjection into the investigated brain nuclei.

2 - RESULTS

2.1. Retrograde tracing

2.1.1. Injection sites. In 10 of 17 rats where tracer migration lasted 5 days the injection was successful, i.e. the Ctb injection was centered at the dLHA, at bregma level -1.80 to -2.16, between the internal capsule and the fornix. This target site is illustrated by the shaded area in Fig. 1. There was no tracer spread to the ventral LHA or to the surrounding brain areas. Ctb-injections considered to be misplaced were either too dorsal, targeting the zona incerta, or extended into the ventral LHA. Five rats with successful intra-dLHA Ctb injections received saline (control) and 5 animals received 20 μg/kg of amylin. Fig. 2A and 2B show schematic drawings of each successful injection site in the dLHA. Fig. 2C shows a photomicrograph with a representative Ctb injection in the dLHA.

Three additional animals were used for an extended tracer migration period of 8 days. Two of these had a successful Ctb injection (not shown).

2.1.2. Projections to dLHA. The total number of c-Fos-positive cells in amylin-injected animals was significantly higher than in controls in all the brain areas analyzed, i.e., the AP (Fig. 2D), NTS, LPB, Ce and BSTL, (Fig. 2E-H and 3). This is consistent with results from previous studies (Rowland et al., 1997; Riediger et al., 2004) demonstrating amylin-induced activation in these brain areas.

Five days after Ctb injection into the dLHA, brown cytoplasmic Ctb labeling was observed in all of the aforementioned areas except the AP, indicating the presence of projecting neurons from those brain areas to the dLHA (Fig. 2D-I). The total number of Ctb-labeled cells did not differ significantly between the amylin and the saline treated groups (Fig. 3).

In animals receiving amylin, 9% of c-Fos positive NTS neurons also showed positive Ctb

labeling, i.e., they projected to the dLHA (Fig. 2E and 3A). From the total number of Ctb-labeled NTS neurons 19% were c-Fos positive in the amylin-treated group. The number of double labeled neurons in amylin-injected animals was significantly higher than in saline-injected controls (Fig. 3A). The highest density of Ctb-labeled neurons was localized in the c-Fos expressing region of the NTS, at the subpostremal level (between bregma -14.28 and -13.70) in the medial and intermediate subnuclei, while there were few cells in the NTSV and NTSDL. No labeled neurons were observed in the commissural subnucleus.

Thirty-three percent of activated neurons in the LPB projected to the dLHA (Fig. 2F, 2I and 3B). This corresponded to 17% of the total number of retrogradely labeled cells in the LPB. The number of double labeled neurons in amylin-injected animals was significantly higher than in controls (Fig. 3B). In the external (LPBE) and crescent (LPBCr) LPB subnuclei, between level -9.00 and -9.36 from bregma, a high density of amylin-activated neurons was observed. At this level of the LPB the highest density of Ctb-labeled neurons was also observed mainly in the LPBE and LPBCr and in the central LPB (LPBC). In the more caudal regions of the parabrachial area (PB, between bregma -9.36 until -9.72), where less amylin-activated neurons were present, Ctb-labeled cells were mainly located in the ventral LPB (LPBV) and medial PB (MPB; not shown).

In the Ce, 4% of the activated neurons were Ctb-positive, and only 2% of the total population of Ctb-positive neurons showed activation (Fig. 2G and 3C). The number of double labeled neurons in amylin-injected animals was not significantly higher than in controls (Fig. 3C). In this brain area, c-Fos expressing neurons were clustered mainly in the capsular division of Ce (starting around bregma -2.04 until -3.12), while most of the Ctb-labeled neurons resided in the medial division of Ce. The only region of colocalization was the lateral Ce.

In the BSTL, 7% of c-Fos positive neurons projected to the dLHA (Fig. 2H and 3D). This corresponded to 4% of the total Ctb-positive neurons in the BSTL. The number of double labeled neurons in amylin-injected animals was not significantly higher than in controls (Fig.

3D). The c-Fos-expressing region was localized between bregma -0.24 and +0.12 in specific BSTL subdivisions (dorsal and posterior subnuclei). Interestingly, the BSTL also showed a high density of Ctb-labeled neurons while the medial BST displayed hardly any Ctb-labeled cells. There were also Ctb-labeled neurons outside the amylin-activated region in the BSTL, that is, caudal to bregma level -0.12 and rostral to level +0.12.

In the two animals that had an extended tracer migration period of 8 days no obvious differences in the pattern of Ctb labeling were found compared to 5 days of tracer migration (not shown).

It has been reported that the retrograde tracer Ctb may also be taken up by fibers of passage and then transported both retrogradely and anterogradely (Chen and Aston-Jones, 1995). In line with such a phenomenon we observed some Ctb-labeled terminals in the more caudal LHA (level -3.48 until -2.64 from bregma) independent of the migration time employed (results not shown). This may suggest anterograde migration of the Ctb tracer after uptake by fibers passing through the injection area in dLHA. Hence, the presence of retrograde tracer signal in the Ce described above may actually result from Ctb uptake by fibers that project from the Ce to the caudal LHA, passing through the targeted dLHA region. The existence of such projections is in line with our (see "anterograde tracing") and previous studies (Ono et al., 1985; Yoshida et al., 2006).

2.1.3. Injections outside dLHA boundaries. In addition to Ctb-injections that were not restricted to the target area, two microinjections largely missed the dLHA but were mainly located in the zona incerta and part of the thalamic reticular nucleus, with just a very small spread into the dLHA in one of these two cases. In these animals there were no positive cells in the AP; the NTS, LPB and BSTL contained generally few (if any) Ctb-positive neurons. Only the Ce nucleus displayed a very high density of Ctb-positive neurons further suggesting that this may result from Ctb uptake by fibers passing thru or dorsally to the dLHA.

2.2. Anterograde tracing

2.2.1. Injection sites. Fig. 4 illustrates the targeted amylin-activated brain areas and specific subnuclei expressing amylin-induced c-Fos. This panel serves as a reference for the BDA injection targets and for the description of projection patterns between amylin-activated brain areas.

Three microinjections in the AP were successful (animals 1-3; see Supplementary Fig. S1). The diffusion field of the tracer tended to spare the marginal subregions but covered most of the AP in the rostrocaudal aspect.

Three NTS injections were successful (animals 4-6). In one of these animals (Fig. 6) there was no tracer spread into the gracile nucleus originating from the pipette tract. The projection pattern observed in this animal was similar to the one observed in the other 2 rats.

See Fig. 6, 7, Supplementary Fig. S1 and S2 for examples of the diffusion fields in the different target areas. Results from one representative example of each injection place are described in detail in the sections below. A summary of the projection density observed after each successful injection is presented in Table 1.

2.2.2. Projections to the dLHA. As expected and consistent with previous studies (Riediger et al., 2004), fasted rats displayed a high number of c-Fos-positive nuclei in the dLHA between bregma -1.80 and -2.16 in the region between the internal capsule and the fornix (see Fig. 7); ad libitum fed animals displayed only few c-Fos-positive nuclei in this area (figure not shown). This dLHA region was analyzed for the presence of BDA-positive fibers. Throughout the manuscript, fibers were analyzed according to the criteria described in the "Evaluation" part of the "Experimental Procedure" section. For examples of the different fiber categories see Fig. 5.

After BDA injection into the AP there were no detectable fibers in the dLHA. BDA injection

into the NTS produced some scattered fibers with several varicosities in the fasting-activated dLHA region (Fig. 6), while the more caudal perifornical LHA area displayed denser terminal fields (not shown).

After BDA injection into the LPB, the c-Fos-positive region of the dLHA close to the fornix displayed dense terminal fields with ample varicosities, as well as fibers of passage (Fig. 7). The region of the dLHA closer to the internal capsule showed several cross-sectioned axons. In contrast to the dLHA, the ventral region of the LHA (not activated by fasting) displayed more fibers of passage and fewer terminals. The caudal regions of the LHA (bregma level -2.40 until -3.48) displayed even higher densities of terminals and fibers of passage, compared with the fasting-activated dLHA (not shown). Fig. 7 shows a double staining of BDA-labeled fibers from the LPB and c-Fos-positive nuclei in the dLHA of a fasted rat. In some cases LPB efferents were in proximity to c-Fos positive neurons in the dLHA; this suggests, though does not prove, that there may be neuronal contacts between LPB projections and fasting activated dLHA neurons.

After BDA injection into the Ce no fibers were detected in the dLHA area where c-Fos is expressed in response to fasting. At this level of the LHA, fiber bundles between the internal capsule and the optic tract were observed, as well as between the internal capsule and the zona incerta. Some cross-sectioned BDA positive axons were located close to the internal capsule, probably belonging to the nigrostriatal bundle. Dense terminal fields were detected in the more caudal LHA region (level -4.20 until -2.64 from bregma), mainly in the ventral and perifornical area. Using extended migration times the same pattern was observed in the caudal LHA, but the density of terminals was somewhat higher. In this case some fibers with few varicosities, which resembled fibers of passage, were observed in the c-Fos expressing dLHA region, together with some cross-sectioned axons (rats 12 and 13, pictures not shown).

BDA injection in the BSTL produced some scattered fibers with several varicosities in the dLHA region expressing c-Fos (Fig. 6). Notably, most areas of the hypothalamus did not

show BDA-labeled fibers, except the rostral LHA. Terminals were seen all over the rostral LHA until level -2.64 from bregma. Interestingly, between level -2.28 and -1.60 they were more numerous mainly in the dorsal subregion containing the dLHA.

2.2.3. Other projections observed. BDA injections also identified projections between amylin-activated areas (Supplementary Fig. S1). These findings are consistent with previous studies using c-Fos immunohistochemistry. We also observed extensive projections from the amylin-activated areas to the other investigated areas of the hypothalamus, namely the arcuate (Arc), ventromedial (VMH), dorsomedial (DMH) and paraventricular (PVH) nucleus of the hypothalamus. These hypothalamic nuclei, which are known to be involved in the control of eating and metabolism, were evaluated to test whether they might also receive input from amylin-activated areas. Namely, NTS injections identified projections to the Arc, DMH and PVH, and LPB injections originated dense projections to the Arc, VMH, DMH, and PVH (Supplementary Fig. S2). For details see Table 1, the Supplementary Results, Fig. S1 and S2.

2.2.4. Injections outside targeted areas. In one rat the BDA-injection missed the target (the AP) but was localized exclusively in the gracile nucleus, i.e. there was no spread into the AP or the NTS. In this case no projections in any of the studied brain regions were observed. This suggests that the observed BDA-labeled NTS and AP efferents to the investigated areas did not originate from the gracile nucleus. Furthermore, retrograde tracing with Ctb indicated that the gracile nucleus does not send projections to the dLHA, as evidenced by the lack of Ctb-positive neuronal bodies in that area after Ctb injection in the dLHA. Therefore, we assume that the BDA-fiber terminals observed in the dLHA originated solely from the NTS.

In one of the animals targeted at the Ce, the injection localized dorsally to the Ce and exclusively in the caudate putamen. In this case there was no labeling in most of the studied regions, except very sparse fibers in the LHA and few fibers also in the LPB. In one of the

animals targeted at the BSTL, the injection localized laterally in the caudate putamen again (in a more rostral portion around level zero from bregma). In this case there was no labeling in any of the analyzed brain areas.

3 - DISCUSSION

In the present study we combined anterograde and retrograde tracing techniques to study the neural connectivity involved in amylin signaling in the rat brain. A major aim was to substantiate the concept that amylin-activated neurons project to the dLHA which is inhibited by amylin. We injected retrograde Ctb tracer into the specific dLHA region and tested if the projecting neurons were specifically activated by amylin as detected by c-Fos expression. There was no statistically significant difference in the number of Ctb single-labeled neurons in each specific area between the control and amylin groups. Therefore, any statistical difference observed in the number of double-labeled cells between the two groups only depended on the amylin-induced change in c-Fos expression, and not on variations of Ctb labeling. To confirm the retrograde tracing outcome we conducted complementary anterograde tracing studies. We investigated whether, after BDA-injections into the amylin activated regions, BDA-labeled fiber terminals could be found in that dLHA subregion and if terminals were in proximity to activated neurons.

The investigation of the neuronal projections from the amylin-activated brain sites distinguishes our work from previous tracing studies with no topographical specificity for amylin-responsive subnuclei (Ricardo and Koh, 1978; Saper and Loewy, 1980; van der Kooy et al., 1984; Shapiro and Miselis, 1985; Cassell et al., 1999; Dong and Swanson, 2004; Geerling and Loewy, 2006). For most of the projections studied here, anterograde and retrograde tracing produced consistent results. Our results showed that the amylin-activated area of the NTS and BSTL project sparsely, while the LPB projects densely to the dLHA subregion where amylin reduces the fasting induced activation. Our findings extend previous studies (Ricardo and Koh, 1978; Kobashi and Adachi, 1988; Li et al., 2005; Hui et al., 2006; Yoshida et al., 2006) and demonstrate that the inputs to the dLHA partly arise from amylin responsive neurons. Many LPB efferents were found in proximity to dLHA c-Fos-positive

nuclei, i.e., neurons that respond to changes in food availability (fasted vs. fed). Whether this close proximity reflects the existence of synapses remains to be confirmed, e.g., by electron microscopy or by the use of trans-synaptic tracing approaches. Of note, we have no definitive proof that the anterogradely labeled terminals in the dLHA after LPB injection originate exclusively in the amylin-activated neurons.

Although we demonstrated BSTL-dLHA projections there was no significant retrograde labeling of amylin-activated neurons in the BSTL. Hence, this pathway does not seem to play an important role in the transmission of the amylin signaling to the dLHA. The NTS may also convey some inhibitory inputs to the dLHA although the projections were less dense than the LPB-dLHA connections. The AP and the amylin-activated area of the Ce do not seem to project directly to the dLHA. Most reports describing the existence of Ce to LHA projections do not distinguish between discrete LHA subregions (Berk and Finkelstein, 1981; Prewitt and Herman, 1998; Yoshida et al., 2006). According to one study by Ono and colleagues (Ono et al., 1985), the Ce mainly projects to mid-rostrocaudal and caudal parts of the LHA. Our present findings are consistent with these results.

In the present study, the AP displayed direct projections to the NTS and LPB (supplementary results), however the relative importance of direct AP-LPB signaling versus the AP-NTS-LPB pathway for amylin's anorectic action is still unknown. Notably, neither the c-Fos nor the feeding studies (Lutz et al., 1998; Lutz et al., 2001; Riediger et al., 2004) that had been conducted previously with AP-lesioned rats differentiate between these pathways because a lesion of the AP unspecifically destroys all efferent AP outflow. Based on the relative density of projections that we identified here, the role of the direct AP-LPB pathway in the mediation of amylin's anorectic effect may have been underestimated until now.

It has been proposed that the NTS sends dense projections to the LHA partly via a synaptic relay in the PB, which may be involved in modulating the activity of the orexinergic and glucose-sensing neurons in the LHA (Williams et al., 2001). Here we describe projections

from the NTS, LPB and perhaps the BSTL to the dLHA subregion that has been shown to be inhibited by amylin (Riediger et al., 2004). Our previous studies suggested that amylin exerts an inhibitory influence on these dLHA neurons, which most likely is synaptically mediated because this region lacks amylin receptors (Sexton et al., 1994; van Rossum et al., 1994; Hilton et al., 1995; Becskei et al., 2004). Since we observed dense projections from the LPB to the dLHA, we propose that the LPB is likely the main candidate area for the transmission of amylin signal from the AP/NTS region to the dLHA, possibly exerting inhibitory effects on LHA neurons.

The phenotype of amylin-activated LPB neurons projecting to the dLHA is not known. The PB contains no glycine-immunoreactive cell bodies (Rampon et al., 1996; Herbert et al., 2000), but contains other inhibitory neuropeptides and neurotransmitters (Sutin and Jacobowitz, 1988). Specifically, there are some γ-aminobutyric acid (GABA)-producing neurons in the LPBE, LPBC and LPBCr (Guthmann et al., 1998; Yokota et al., 2007), i.e. subregions of the LPBN that are activated by amylin. Interestingly, it has recently been reported that activation of LHA GABA-A receptors suppresses feeding and induces body weight loss in rats (Turenius et al., 2009). Hence, GABA may also play a role in the suppression of neuronal dLHA activity by amylin. The existence of a high percentage of amylin activated neurons directly projecting to the dLHA is in principle in line with such a direct mechanism of inhibition. We cannot exclude the possibility that GABAergic interneurons in the LHA (Gao and van den Pol, 2001), or in other brain areas, indirectly mediate the amylin-dependent inhibition of dLHA neurons. Since there is no evidence that amylin induces c-Fos expression in the LHA it appears less likely that an activation of local LHA inhibitory interneurons might play a major role in this respect. Further neurophysiological studies are required to identify the neurotransmitter or neuropeptide mediating the inhibition of dLHA neurons.

The phenotype of the fasting-activated dLHA neurons is presently not known. Orexin-

containing neurons are predominantly located in the medial and caudal LHA, and up to 33% of them show activation in response to insulin-induced hypoglycemia (Moriguchi et al., 1999). However, at the most rostral levels, particularly at the dLHA, only a few orexin-positive cells are scattered around the fornix (Broberger et al., 1998; Swanson et al., 2005). Furthermore, we have unpublished observation from rats indicating no colocalization between orexin and fasting-activated neurons in the rat dLHA. We recently reported the same observation in a corresponding dLHA area of mice, in which orexin expressing neurons were completely absent in that particular region (Becskei et al., 2009). It is also known that neurons activated by insulin-induced hypoglycemia do not express MCH (Moriguchi et al., 1999).

Extending previous reports (Ricardo and Koh, 1978; Saper and Loewy, 1980; Bester et al., 1997; Prewitt and Herman, 1998), we furthermore identified specific projections from amylin-activated subnuclei to hypothalamic areas involved in the control of eating and energy balance (supplementary results). These include projections from the NTS and the LPB to the Arc, PVH and DMH. Dense projections also existed from the LPB to the VMH. We observed projections from the Ce to the DMH and PVH, but not to the VMH (Ono et al., 1985; Prewitt and Herman, 1998).

3.1. Functional considerations

The dose of amylin employed in the present study was previously shown to attenuate fasting-induced activation of the dLHA (Riediger et al., 2004). It needs to be stressed that this dose of amylin is supraphysiological and produces plasma amylin concentrations that are higher than the one observed after a meal (Young, 2005). However, refeeding, i.e. 2h-access to food after a 24h-food deprivation period, not only reduces the fasting-induced c-Fos response in the dLHA, but it also induces neuronal activation in the AP and NTS (Riediger et al., 2004). The amylin receptor antagonist AC187 given before refeeding was able to block the refeeding induced activation of the AP (Riediger et al., 2004). Taken together, this suggests that the

feeding induced release of endogenous amylin contributes to the neuronal activation of the AP in refed animals. Therefore, even though the effects induced by amylin have been produced at supraphysiological amylin levels, it appears plausible that endogenous amylin may also contribute to the feeding-related suppression of dLHA activity via the AP-NTS-LPB pathway. Despite the immunohistological evidence that amylin inhibits dLHA activity, so far no behavioral study directly investigated whether the dLHA is functionally involved in amylin's anorectic effect. LHA neuronal activity has been suggested to be closely associated with the onset of feeding, and inhibition of lateral hypothalamic neurons by glucose is sufficient to suppress feeding (Booth, 1968; Kurata et al., 1986; Bernardis and Bellinger, 1996; Zhang et al., 2005). Hence amylin's inhibition of dLHA neurons may be involved in the reduction of food intake after peripheral amylin. A role of the amylin-inhibited dLHA neurons in the control of eating is supported by the observation mentioned above that refeeding also leads to a reversal of fasting-induced activation of dLHA neurons (Riediger et al., 2004).

In our study we also found extensive projections from amylin-activated areas, particularly the NTS, LPB and Ce to hypothalamic centers that, among other functions, are involved in the control of eating and energy balance. Among the former structures the LPB clearly showed the strongest efferent projections to the hypothalamus. Interestingly, recent studies suggest that amylin interacts with leptin, possibly at the level of the VMH and the Arc. Amylin pre-treatment partially restored hypothalamic leptin sensitivity in leptin resistant diet-induced obese rats in the VMH (Roth et al., 2008) and increased leptin sensitivity also in lean rats (Turek et al., 2010). These effects have been suggested to depend on polysynaptic connections from the AP to the VMH and the Arc (Roth et al., 2008; Turek et al., 2010). Our demonstration of very dense projections from the amylin-activated LPB region to the VMH and the Arc (Supplementary Results and Fig. S2) strongly supports such a mechanism.

3.2. Final remarks

Amylinomimetic agents alone or in combination with other hormones, especially leptin, are presently being evaluated in clinical trials in obese subjects, yielding promising results as anti-obesity treatments. Amylinomimetics are already used to improve blood glucose profiles in diabetic patients (Weyer et al., 2001; Hollander et al., 2004). A detailed knowledge about amylin's central nervous signaling pathways is therefore not only important to understand the mechanisms of amylin action but also for the development of therapeutic strategies against obesity and associated metabolic disorders. Particularly amylin's effect on the hypothalamic network has until recently been poorly understood, but it may be fundamental to develop future efficient therapeutic approaches to treat obesity.

Based on neuronal connectivity, we suggest that the LPB seems to be the important structure to transmit the amylin signal from the AP/NTS region to the dLHA, therefore probably mediating the previously reported amylin-induced inhibition of dLHA (Riediger et al., 2004). Previous lesion studies showed that there is an amylin-induced excitatory signal transduction originating in the AP, being propagated to rostral brain sites (Rowland and Richmond, 1999; Riediger et al., 2004; Becskei et al., 2007). Based upon the present tracing studies and the previous lesion studies, we propose that the LPB may function as a key relay site for the transmission of amylin signaling from the hindbrain to the forebrain.

4 - EXPERIMENTAL PROCEDURE

Animals

Seventy-eight (20 for the retrograde tracing study and 58 for the anterograde tracing study) adult male Wistar rats (Elevage Janvier, Le-Genest-St. Isle, France) weighing between 270-300g at the time of stereotaxic surgery were used. Additionally, 2 rats that were not subjected to surgery were used as reference to identify and illustrate the typical amylin-induced neuronal-activation pattern, as gauged by c-Fos expression, in the rat brain. The animals were housed in individual wire-mesh cages (50x25x18 cm) and maintained in a temperature-controlled room on an artificial 12:12h dark-light cycle (21 ± 1°C, lights on from 3:00 to 15:00). Rats had ad libitum access to water and standard laboratory rat chow (890 25 W16; Provimi Kliba, Gossau, Switzerland), except during food deprivation as described below. All rats were handled and habituated to the investigator and to the housing conditions for at least one week before surgery and at least two weeks before perfusion. The animals used were acquired and maintained in accordance with the European Communities Council Directive of 24 November 1986 (86/609/EEC) and procedures were approved by the Veterinary Office of the Canton Zurich, Switzerland.

Retrograde tracing

The tracing methods were adapted from studies using similar methodology (Pouzet et al., 1999; Kriegsfeld et al., 2004). Injections of the retrograde tracer cholera toxin B subunit (Ctb; #104 lot 10427B1, List Biological Laboratories; Campbell, USA) were made to visualize afferents of the dLHA. Under isoflurane anesthesia the rats' skull was fixed in a stereotaxic frame and the injection of 1% Ctb solution (dissolved in sterile pyrogen-free distilled water) was performed by microinjection with a pneumatic injector (Picospritzer III, General Valve,

NJ, USA), according to the stereotactic coordinates of Paxinos and Watson (Paxinos and Watson, 2007) (using bregma as reference point; dorsoventral: –8.3 mm; lateromedial: +1.9 mm; rostrocaudal: –1.8 mm). The injections were specifically targeted to the dLHA area that is activated by fasting (between -1.80 and -2.16 from bregma) and where the fasting-induced c-Fos expression is attenuated by amylin (Riediger et al., 2004). This target site is illustrated by the shaded area in Fig. 1. Only injections restricted to the dLHA, with no or minimal spread into the ventral LHA or other surrounding areas were considered successful. The glass pipettes used for injection had an inner diameter of 20 μm and the injections were performed in 4 pulses of 10 msec at 4 min intervals and using a pressure of 40 psi. Four days after surgery the animals were fasted starting at dark onset. Twenty-four hours later (5 days after tracer injection) they were subcutaneously injected with either saline (control) or amylin (20μg/kg; Bachem, Dubendorf, Switzerland). The rats were deeply anesthetized, followed by transcardial perfusion 2h after injection, as described below. No food was offered between injection and sacrifice. This time point was chosen based on reports that show that c-Fos expression peaks between 60 and 90min after neuronal activation (Hoffman et al., 1993). Three additional rats were allowed a tracer migration period of 8 instead of 5 days. The migration period was chosen according to literature (Cobos et al., 2003; Gamboa-Esteves et al., 2004; Kriegsfeld et al., 2004) and previous own pilot experiments assessing optimal time for tracer transport.

Anterograde tracing

Injections of the anterograde tracer biotinylated dextran-amine (BDA, amine group is a lysine, # B9139 lot 125K1219, 10’000 MW, Sigma-Aldrich Chemie GmbH, Buchs, Switzerland) (Reiner et al., 2000) were used to confirm the projections detected by the retrograde tracing study, and to identify further neuronal pathways originating from amylin activated brain structures. Only BDA microinjections targeting a considerable area of the amylin-activated

subnuclei, with no or minimal tracer spread into surrounding areas were considered successful. For AP or NTS injections, the animals were anaesthetized by intraperitoneal injection of a mixture of ketamine hydrochloride (77 mg/kg) and xylazine hydrochloride (8 mg/kg) and their skull was fixed in the stereotaxic frame flexed ventrally in an almost right-angled position. The skin and muscles of the neck were cut in the midline and the nuchal musculature was bluntly dissected to expose the atlanto-occipital membrane. The membrane was excised to reveal the obex and the adjacent AP. A 10% solution of BDA (dissolved in sterile phosphate buffer pH 7.5, Sigma-Aldrich) was microinjected into the AP or the NTS with the pneumatic injector (AP: 0.5 mm rostral to obex and 0.3 mm ventral from surface; NTS: 0.5 mm rostral to obex, +0.6 mm lateral and 0.6 mm ventral from surface). The glass pipettes used for injection had an inner diameter of 40 μm and the injections were performed at a pressure of 40 psi with 5 msec pulse duration, giving 3 pulses in 4 min intervals.

For LPB, Ce or BSTL injections, the same approach as for LHA injection was employed (see "Retrograde tracing"), but using the following coordinates with bregma as reference: Ce, dorsoventral: –8.0 mm, lateromedial: +4.5 mm, rostrocaudal: –2.3 mm; BSTL, dorsoventral: –6.5 mm, lateromedial: +1.5 mm, rostrocaudal: 0.0 mm; LPB, using a 24^{o} forward injection angle, dorsoventral: –7.4 mm, lateromedial: +2.2 mm, rostrocaudal: -6.15 mm. The glass pipettes had an inner diameter of 40 μm and the injections were performed at 40 psi with 10 msec pulse duration, applying 3 pulses (4 pulses in the Ce) in 4 min intervals. The different pulse number and duration for the different brain areas were chosen to adjust the injection volume to the size of target areas and were based on pilot studies. Tracer injections targeting the NTS were intended to cover the subpostremal level of the NTS (-13.68 to -14.28 from bregma), covering mainly the intermediate (NTSIM) and medial (NTSM) parts sparing both the interstitial and commissural (NTSC) subnuclei (Fig. 4) and also the dorsal motor nucleus of the vagus (DMX). The diffusion field of the tracer in the LPB included the LPBE, LPBC, LPBV and LPBCr subnuclei, (level -9.00 to -9.60 from bregma) (Fig. 4). Injections targeting

the Ce aimed at bregma level -2.28 to -3.00 and injections aiming at the BSTL targeted the latero-posterior (BSTLP) and latero-dorsal (BSTLD) subdivisions only (level +0.12 to -0.12). Microinjections that missed their target, but were specifically located in surrounding areas, were also evaluated to investigate whether they would label the same brain areas as the correctly targeted injections. This was particularly important to exclude the possibility that the BDA-labeled fibers observed in the analyzed areas originate from areas surrounding the target site.

The migration times were chosen according to literature (Pickel and Colago, 1999; Cobos et al., 2003; Tsumori et al., 2006) and own pilot experiments: 11 days for the AP, the NTS and the BSTL; 9 days for the LPB and 7 days for Ce. The aim was to find an optimal time period that would allow the visualization of the projecting fibers in the various areas of interest. In addition, a tracer migration period of 14 days was used in some animals to exclude that a lack of BDA-signal particularly in more distant projection areas could have been due to an insufficient migration time.

Before sacrifice the rats were food deprived for 24h starting at dark onset to induce c-Fos expression in the dLHA. Control animals were fed ad libitum during the same time period. Two hours into the next dark phase the rats were perfused as described below. For every experiment fasted and ad libitum animals were processed in parallel.

Perfusion and Immunohistochemistry

Two hours after dark onset the animals were deeply anaesthetized (pentobarbital sodium, 100mg/kg i.p., Kantonsapotheke Zürich, Switzerland) and transcardially perfused with ice-cold sodium phosphate buffer (PB 0.1 M, pH 7.2), followed by 4% paraformaldehyde in PB. Brains were postfixed for 2h and cryoprotected in 20% sucrose/PB (48h at 4°C). Coronal 20 µm thick brain sections containing the AP, NTS, LPB, Ce, LHA and the BSTL (according to (Paxinos and Watson, 2007) were cut in a cryostat at -20^{o}C (Leica CM3050S, Nussloch,

Germany), and thaw mounted on adhesive glass slides (SuperFrost Plus, Menzel, Germany).

For Ctb and c-Fos double labeling, the brain slices were first stained for Ctb and then for c-Fos using a double 3,3'-diaminobenzidine-tetrahydrochloride substrate (DAB) method. After air drying for 1h at room temperature and rehydration in phosphate-buffered saline (pH 7.4) containing 0.1% Triton X-100 (PBST), the sections were incubated in donkey normal serum (1.5% in 0.3% PBST; Jackson ImmunoResearch) for 2h, followed by polyclonal goat anti-cholera toxin B (choleragenoid) subunit antibody (1:15 000 in 0.3% PBST; #703, lot 7032A3, List Biological Laboratories Inc, USA) for 48h at 4^{o}C. The sections were then incubated in biotin-SP-conjugated donkey anti-goat IgG (H+L) (1:1 000 in 0.3% PBST, #705-065-147, lot 67752, Jackson ImmunoResearch Inc, UK) for 90 min at room temperature. After incubation for 1h in 1:100 avidin-biotin-peroxidase complex (Vectastain ABC kit, Vector), Ctb-labeled cells were stained by incubation for 3 min in DAB solution prepared in Tris-HCl buffer pH 7.6 (0.05% DAB, 0.008% H_2O_2, Sigma-Aldrich). After washing in PBST the slides were then incubated in 1.5% donkey normal serum for 1h, followed by a 48h incubation in the primary rabbit anti-c-Fos IgG fraction of antiserum against peptide corresponding to the N-terminal region of c-Fos (1:10 000 in 0.3% PBST; #F7799, lot 124K4881 and 115K4751, Sigma-Aldrich, USA) at 4^{o}C. A biotin-SP-conjugated donkey anti-rabbit IgG (H+L) secondary antibody was used (1:1 000, #711-065-152, lot 68226, Jackson ImmunoResearch) for 90 min at room temperature. After incubation for 1h in 1:100 ABC, c-Fos was visualized by incubation for 7 min in nickel-cobalt enhanced DAB solution in Tris-HCl (0.05% DAB, 0.008% H_2O_2, 0.08% $NiCl_2$, and 0.01% $CoCl_2$, Sigma-Aldrich). The slides were rinsed in PBS, dehydrated in graded alcohol, immersed in xylol, and cover-slipped with Entellan (Merck, Germany).

For double-labeling of BDA-positive fibers and fasting-induced c-Fos-positive nuclei in the dLHA, fluorescence immunohistochemistry (c-Fos) and a DAB staining (BDA) were combined. The fluorescent c-Fos detection method was preferred over the DAB method to

reduce background staining that might interfere with the detection of thin BDA-labeled fibers in the dLHA. After air drying and rehydration in PBST, the sections were incubated for 1h in 1:100 ABC, and then incubated 7 min in nickel-cobalt enhanced DAB in Tris-HCl (see above). After washing in PBST the slides were incubated in 1.5% donkey normal serum for 1h to block unspecific binding, then for 48h in the same primary rabbit anti-c-Fos IgG antibody as above (1:2 000 in 0.3% PBST; #F7799, lot 124K4881 and 115K4751, Sigma-Aldrich, USA) at 4^{o}C. After washing the sections were incubated for 75 min at room temperature in Alexa Fluorophore 555-labeled donkey anti-rabbit IgG (H+L) (1:250 in 0.3% PBST, #A31572, lot 52636A, Invitrogen), rinsed in PBS and mounted with Citifluor mounting medium (PBS/glycerol 1:1; Citifluor Products, UK).

The specificity of the primary antibodies was demonstrated by the respective suppliers and was confirmed by own controls. Specifically, the anti-Ctb antibody was raised in goat against the whole purified Cholera B Subunit used for tracing. The B-subunit is a 11 kDa peptide which forms a 55 kDa pentamer. The specificity of the antibody was tested by immunoprecipitation. The anti-c-Fos antibody used identifies c-Fos by immunoblotting as single or multiple bands at 50-62 kDa, and bands of 40 kDa representing c-Fos degradation products. This antibody was raised against the N-terminal region of human c-Fos (aminoacids 3-16 with a C-terminal added lysine: FSGFNADYEASSSR-K) which is a region identical in rat, mouse and pig c-Fos protein. Staining of c-Fos by this antibody is specifically inhibited with c-Fos immunizing peptide. The specificity of the secondary antibodies was demonstrated by the respective suppliers through immunoelectrophoresis. They were tested by ELISA or were solid-phase adsorbed to ensure minimal cross-reactivity with serum proteins from other species. The lack of unspecific tissue binding was further verified by control immunostainings omitting the primary antibody.

Two animals were used to illustrate the typical amylin-induced neuronal activation pattern in the brain; they were injected with 20 μg/kg amylin subcutaneously after 24h of fasting

starting at dark onset, and were perfused 2h later as described. A single immunohistochemical reaction against c-Fos protein using nickel-cobalt enhanced DAB detection was performed as described above.

Evaluation

Brain sections were analyzed using a microscope equipped with a digital camera (Axioskop, Carl Zeiss, Switzerland). The injection sites were evaluated at 5x and 10x magnification and photomicrographs were taken. In the retrograde tracing study Ctb-labeled neurons were analyzed in the areas showing c-Fos in response to amylin. For quantification of the total number of c-Fos, Ctb and c-Fos/Ctb double-immunoreactive neurons on the ipsilateral side of the injection area, every third section of each brain area was analyzed, in a blinded fashion to treatment, resulting in 7-10 slices per area and animal (AP and NTS, bregma -13.68 to -14.28; LPB, bregma -9.00 to -9.48; Ce, bregma -2.28 to -3.00). Every second section of the BSTL subdivision, between level +0.12 and -0.12, was evaluated (7 slices in total). The cell counts from the successful Ctb injections of amylin and saline-injected rats were averaged for each area per animal. Group mean values ± standard error, were calculated from these averaged cell counts.

In the anterograde tracing study, the presence of BDA-labeled fibers in the c-Fos expressing area of the dLHA (Fig. 1) was evaluated. A semi-quantitative evaluation of the BDA-labeled fibers was conducted for the AP, NTS, LPB, Ce, BSTL, dLHA and further hypothalamic nuclei, namely the Arc, VMH, DMH and PVH. Use of 20x and 40x magnifications allowed to identify linear and ramified fibers with sparse or abundant varicosities; examples of each are presented in Fig. 5. These criteria have been used before to distinguish different axonal morphologies (Debanne, 2004; Kriegsfeld et al., 2004). We adapted these classifications and defined fibers of passage as fibers carrying sparse, scattered varicosities and no arborizations or ramifications (Fig. 5A). Dense fiber arborizations (Fig. 5C) and linear fibers with abundant

varicosities (also known as “bead-on-a-string” fibers; Fig. 5B) were considered to be terminals. For semi-quantitative evaluation of fiber density we used an arbitrary scale: (+) presence of very sparse fibers scattered in the nucleus, + presence of sparse fibers consistently throughout the nucleus, ++ dense, +++ very dense and ++++ extensive fiber terminals (see Table 1). Pictures of c-Fos immunofluorescence and BDA immunoreactivity (DAB) were taken from the same position in the slice to illustrate the proximity between c-Fos positive nuclei and BDA labeled fibers. In order to better visualize the position of c-Fos neurons in relation to BDA-positive fibers labeled in black DAB, grayscale images from c-Fos fluorescence immunostainings were inverted using the software Adobe Photoshop, so that c-Fos nuclei appear dark on a light background. Photomicrographs of the typical amylin induced c-Fos expression pattern are presented in Fig. 4.

All images and figure panels were prepared using the software Corel Draw 12 or Adobe Photoshop, and small adjustments of the brightness and contrast were made in some pictures for adequate printing quality. All brain schemes were reproduced or adapted with permission from The Rat Brain in Stereotaxic Coordinates (Paxinos and Watson, 2007).

Statistics

Statistical comparisons were done by Student’s t-test on parametric data and by Mann-Whitney Rank Sum test for non-parametric comparisons. Differences were considered significant with $p<0.05$.

ACKNOWLEDGEMENTS

The authors thank Prof. Hans-Rudolph Berthoud from the Pennington Biomedical Research Center in Louisiana and Prof. Wolfgang Langhans from the Institute of Animal Sciences in ETH Zurich for their valuable input during the development of the present study.

C.S. Potes was supported by the Novartis Foundation for Medical and Biological Research (grant number 07C66, PI Thomas Lutz). This study was supported by the Swiss National Research Foundation (grant number 109222).

REFERENCES

Aronne, L., Fujioka, K., Aroda, V., Chen, K., Halseth, A., Kesty, N. C., Burns, C., Lush, C. W., Weyer, C., 2007. Progressive reduction in body weight after treatment with the amylin analog pramlintide in obese subjects: a phase 2, randomized, placebo-controlled, dose-escalation study. J Clin Endocrinol Metab. 92**,** 2977-83.

Barth, S. W., Riediger, T., Lutz, T. A., Rechkemmer, G., 2003. Differential effects of amylin and salmon calcitonin on neuropeptide gene expression in the lateral hypothalamic area and the arcuate nucleus of the rat. Neurosci Lett. 341**,** 131-4.

Beaumont, K., Kenney, M. A., Young, A. A., Rink, T. J., 1993. High affinity amylin binding sites in rat brain. Mol Pharmacol. 44**,** 493-7.

Becskei, C., Grabler, V., Edwards, G. L., Riediger, T., Lutz, T. A., 2007. Lesion of the lateral parabrachial nucleus attenuates the anorectic effect of peripheral amylin and CCK. Brain Res. 1162**,** 76-84.

Becskei, C., Lutz, T. A., Riediger, T., 2009. Blunted fasting-induced hypothalamic activation and refeeding hyperphagia in late onset obesity. Neuroendocrinology. (in press).

Becskei, C., Riediger, T., Zund, D., Wookey, P., Lutz, T. A., 2004. Immunohistochemical mapping of calcitonin receptors in the adult rat brain. Brain Res. 1030**,** 221-33.

Berk, M. L., Finkelstein, J. A., 1981. Afferent projections to the preoptic area and hypothalamic regions in the rat brain. Neuroscience. 6**,** 1601-24.

Bernardis, L. L., Bellinger, L. L., 1996. The lateral hypothalamic area revisited: ingestive behavior. Neurosci Biobehav Rev. 20**,** 189-287.

Bester, H., Besson, J. M., Bernard, J. F., 1997. Organization of efferent projections from the parabrachial area to the hypothalamus: a Phaseolus vulgaris-leucoagglutinin study in the rat. J Comp Neurol. 383**,** 245-81.

Booth, D. A., 1968. Effects of intrahypothalamic glucose injection on eating and drinking elicited by insulin. J Comp Physiol Psychol. 65**,** 13-6.

Broberger, C., De Lecea, L., Sutcliffe, J. G., Hokfelt, T., 1998. Hypocretin/orexin- and melanin-concentrating hormone-expressing cells form distinct populations in the rodent lateral hypothalamus: relationship to the neuropeptide Y and agouti gene-related protein systems. J Comp Neurol. 402**,** 460-74.

Butler, P. C., Chou, J., Carter, W. B., Wang, Y. N., Bu, B. H., Chang, D., Chang, J. K., Rizza, R. A., 1990. Effects of meal ingestion on plasma amylin concentration in NIDDM and nondiabetic humans. Diabetes. 39**,** 752-6.

Cassell, M. D., Freedman, L. J., Shi, C., 1999. The intrinsic organization of the central extended amygdala. Ann N Y Acad Sci. 877**,** 217-41.

Chen, S., Aston-Jones, G., 1995. Evidence that cholera toxin B subunit (CTb) can be avidly taken up and transported by fibers of passage. Brain Res. 674**,** 107-11.

Cobos, A., Lima, D., Almeida, A., Tavares, I., 2003. Brain afferents to the lateral caudal ventrolateral medulla: a retrograde and anterograde tracing study in the rat. Neuroscience. 120**,** 485-98.

Debanne, D., 2004. Information processing in the axon. Nat Rev Neurosci. 5**,** 304-16.

Dong, H. W., Swanson, L. W., 2004. Organization of axonal projections from the anterolateral area of the bed nuclei of the stria terminalis. J Comp Neurol. 468**,** 277-98.

Gamboa-Esteves, F. O., McWilliam, P. N., Batten, T. F., 2004. Substance P (NK1) and somatostatin (sst2A) receptor immunoreactivity in NTS-projecting rat dorsal horn neurones activated by nociceptive afferent input. J Chem Neuroanat. 27**,** 251-66.

Gao, X. B., van den Pol, A. N., 2001. Melanin concentrating hormone depresses synaptic activity of glutamate and GABA neurons from rat lateral hypothalamus. J Physiol. 533**,** 237-52.

Geerling, J. C., Loewy, A. D., 2006. Aldosterone-sensitive neurons in the nucleus of the solitary tract: efferent projections. J Comp Neurol. 497**,** 223-50.

Guthmann, A., Fritschy, J. M., Ottersen, O. P., Torp, R., Herbert, H., 1998. GABA, GABA transporters, GABA(A) receptor subunits, and GAD mRNAs in the rat parabrachial and Kolliker-Fuse nuclei. J Comp Neurol. 400**,** 229-43.

Herbert, H., Guthmann, A., Zafra, F., Ottersen, O. P., 2000. Glycine, glycine receptor subunit and glycine transporters in the rat parabrachial and Kolliker-Fuse nuclei. Anat Embryol (Berl). 201**,** 259-72.

Hilton, J. M., Chai, S. Y., Sexton, P. M., 1995. In vitro autoradiographic localization of the calcitonin receptor isoforms, C1a and C1b, in rat brain. Neuroscience. 69**,** 1223-37.

Hoffman, G. E., Smith, M. S., Verbalis, J. G., 1993. c-Fos and related immediate early gene products as markers of activity in neuroendocrine systems. Front Neuroendocrinol. 14**,** 173-213.

Hollander, P., Maggs, D. G., Ruggles, J. A., Fineman, M., Shen, L., Kolterman, O. G., Weyer, C., 2004. Effect of pramlintide on weight in overweight and obese insulin-treated type 2 diabetes patients. Obes Res. 12**,** 661-8.

Hui, R., Chen, T., Li, Y. Q., 2006. The reciprocal connections of endomorphin 1- and endomorphin 2-containing neurons between the hypothalamus and nucleus tractus solitarii in the rat. Neuroscience. 138**,** 171-81.

Kobashi, M., Adachi, A., 1988. A direct hepatic osmoreceptive afferent projection from nucleus tractus solitarius to dorsal hypothalamus. Brain Res Bull. 20**,** 487-92.

Kriegsfeld, L. J., Leak, R. K., Yackulic, C. B., LeSauter, J., Silver, R., 2004. Organization of suprachiasmatic nucleus projections in Syrian hamsters (Mesocricetus auratus): an anterograde and retrograde analysis. J Comp Neurol. 468**,** 361-79.

Kurata, K., Fujimoto, K., Sakata, T., Etou, H., Fukagawa, K., 1986. D-glucose suppression of eating after intra-third ventricle infusion in rat. Physiol Behav. 37**,** 615-20.

Li, C. S., Cho, Y. K., Smith, D. V., 2005. Modulation of parabrachial taste neurons by electrical and chemical stimulation of the lateral hypothalamus and amygdala. J Neurophysiol. 93**,** 1183-96.

Lutz, T. A., 2005. Pancreatic amylin as a centrally acting satiating hormone. Curr Drug Targets. 6**,** 181-9.

Lutz, T. A., Geary, N., Szabady, M. M., Del Prete, E., Scharrer, E., 1995. Amylin decreases meal size in rats. Physiol Behav. 58**,** 1197-202.

Lutz, T. A., Mollet, A., Rushing, P. A., Riediger, T., Scharrer, E., 2001. The anorectic effect of a chronic peripheral infusion of amylin is abolished in area postrema/nucleus of the solitary tract (AP/NTS) lesioned rats. Int J Obes Relat Metab Disord. 25**,** 1005-11.

Lutz, T. A., Senn, M., Althaus, J., Del Prete, E., Ehrensperger, F., Scharrer, E., 1998. Lesion of the area postrema/nucleus of the solitary tract (AP/NTS) attenuates the anorectic effects of amylin and calcitonin gene-related peptide (CGRP) in rats. Peptides. 19**,** 309-17.

Moriguchi, T., Sakurai, T., Nambu, T., Yanagisawa, M., Goto, K., 1999. Neurons containing orexin in the lateral hypothalamic area of the adult rat brain are activated by insulin-induced acute hypoglycemia. Neurosci Lett. 264**,** 101-4.

Ogawa, A., Harris, V., McCorkle, S. K., Unger, R. H., Luskey, K. L., 1990. Amylin secretion from the rat pancreas and its selective loss after streptozotocin treatment. J Clin Invest. 85**,** 973-6.

Ono, T., Luiten, P. G., Nishijo, H., Fukuda, M., Nishino, H., 1985. Topographic organization of projections from the amygdala to the hypothalamus of the rat. Neurosci Res. 2**,** 221-38.

Paxinos, G., Watson, C., 2007. The rat brain in stereotaxic coordinates, vol. Academic Press, Oxford.

Pickel, V. M., Colago, E. E., 1999. Presence of mu-opioid receptors in targets of efferent projections from the central nucleus of the amygdala to the nucleus of the solitary tract. Synapse. 33**,** 141-52.

Pouzet, B., Veenman, C. L., Yee, B. K., Feldon, J., Weiner, I., 1999. The effects of radiofrequency lesion or transection of the fimbria-fornix on latent inhibition in the rat. Neuroscience. 91**,** 1355-68.

Prewitt, C. M., Herman, J. P., 1998. Anatomical interactions between the central amygdaloid nucleus and the hypothalamic paraventricular nucleus of the rat: a dual tract-tracing analysis. J Chem Neuroanat. 15**,** 173-85.

Rampon, C., Luppi, P. H., Fort, P., Peyron, C., Jouvet, M., 1996. Distribution of glycine-immunoreactive cell bodies and fibers in the rat brain. Neuroscience. 75**,** 737-55.

Reiner, A., Veenman, C. L., Medina, L., Jiao, Y., Del Mar, N., Honig, M. G., 2000. Pathway tracing using biotinylated dextran amines. J Neurosci Methods. 103**,** 23-37.

Ricardo, J. A., Koh, E. T., 1978. Anatomical evidence of direct projections from the nucleus of the solitary tract to the hypothalamus, amygdala, and other forebrain structures in the rat. Brain Res. 153**,** 1-26.

Riediger, T., Schmid, H. A., Lutz, T., Simon, E., 2001. Amylin potently activates AP neurons possibly via formation of the excitatory second messenger cGMP. Am J Physiol Regul Integr Comp Physiol. 281**,** R1833-43.

Riediger, T., Zuend, D., Becskei, C., Lutz, T. A., 2004. The anorectic hormone amylin contributes to feeding-related changes of neuronal activity in key structures of the gut-brain axis. Am J Physiol Regul Integr Comp Physiol. 286**,** R114-22.

Roth, J. D., Roland, B. L., Cole, R. L., Trevaskis, J. L., Weyer, C., Koda, J. E., Anderson, C. M., Parkes, D. G., Baron, A. D., 2008. Leptin responsiveness restored by amylin agonism in diet-induced obesity: evidence from nonclinical and clinical studies. Proc Natl Acad Sci U S A. 105**,** 7257-62.

Rowland, N. E., Crews, E. C., Gentry, R. M., 1997. Comparison of Fos induced in rat brain by GLP-1 and amylin. Regul Pept. 71**,** 171-4.

Rowland, N. E., Richmond, R. M., 1999. Area postrema and the anorectic actions of dexfenfluramine and amylin. Brain Res. 820**,** 86-91.

Saper, C. B., 2002. The central autonomic nervous system: conscious visceral perception and autonomic pattern generation. Annu Rev Neurosci. 25**,** 433-69.

Saper, C. B., Loewy, A. D., 1980. Efferent connections of the parabrachial nucleus in the rat. Brain Res. 197**,** 291-317.

Sexton, P. M., Paxinos, G., Kenney, M. A., Wookey, P. J., Beaumont, K., 1994. In vitro autoradiographic localization of amylin binding sites in rat brain. Neuroscience. 62**,** 553-67.

Shapiro, R. E., Miselis, R. R., 1985. The central neural connections of the area postrema of the rat. J Comp Neurol. 234**,** 344-64.

Smith, S. R., Blundell, J. E., Burns, C., Ellero, C., Schroeder, B. E., Kesty, N. C., Chen, K. S., Halseth, A. E., Lush, C. W., Weyer, C., 2007. Pramlintide treatment reduces 24-h caloric intake and meal sizes and improves control of eating in obese subjects: a 6-wk translational research study. Am J Physiol Endocrinol Metab. 293**,** E620-7.

Sutin, E. L., Jacobowitz, D. M., 1988. Immunocytochemical localization of peptides and other neurochemicals in the rat laterodorsal tegmental nucleus and adjacent area. J Comp Neurol. 270**,** 243-70.

Swanson, L. W., Sanchez-Watts, G., Watts, A. G., 2005. Comparison of melanin-concentrating hormone and hypocretin/orexin mRNA expression patterns in a new parceling scheme of the lateral hypothalamic zone. Neurosci Lett. 387**,** 80-4.

Tsumori, T., Yokota, S., Kishi, T., Qin, Y., Oka, T., Yasui, Y., 2006. Insular cortical and amygdaloid fibers are in contact with posterolateral hypothalamic neurons projecting to the nucleus of the solitary tract in the rat. Brain Res. 1070**,** 139-44.

Turek, V. F., Trevaskis, J. L., Levin, B. E., Dunn-Meynell, A. A., Irani, B., Gu, G., Wittmer, C., Griffin, P. S., Vu, C., Parkes, D. G., Roth, J. D., 2010. Mechanisms of Amylin/Leptin Synergy in Rodent Models. Endocrinology. 151**,** 143-152.

Turenius, C. I., Htut, M. M., Prodon, D. A., Ebersole, P. L., Ngo, P. T., Lara, R. N., Wilczynski, J. L., Stanley, B. G., 2009. GABA(A) receptors in the lateral hypothalamus as mediators of satiety and body weight regulation. Brain Res. 1262**,** 16-24.

van der Kooy, D., Koda, L. Y., McGinty, J. F., Gerfen, C. R., Bloom, F. E., 1984. The organization of projections from the cortex, amygdala, and hypothalamus to the nucleus of the solitary tract in rat. J Comp Neurol. 224**,** 1-24.

van Rossum, D., Menard, D. P., Fournier, A., St-Pierre, S., Quirion, R., 1994. Autoradiographic distribution and receptor binding profile of [125I]Bolton Hunter-rat amylin binding sites in the rat brain. J Pharmacol Exp Ther. 270**,** 779-87.

Weyer, C., Maggs, D. G., Young, A. A., Kolterman, O. G., 2001. Amylin replacement with pramlintide as an adjunct to insulin therapy in type 1 and type 2 diabetes mellitus: a physiological approach toward improved metabolic control. Curr Pharm Des. 7**,** 1353-73.

Williams, G., Bing, C., Cai, X. J., Harrold, J. A., King, P. J., Liu, X. H., 2001. The hypothalamus and the control of energy homeostasis: different circuits, different purposes. Physiol Behav. 74**,** 683-701.

Yokota, S., Oka, T., Tsumori, T., Nakamura, S., Yasui, Y., 2007. Glutamatergic neurons in the Kolliker-Fuse nucleus project to the rostral ventral respiratory group and phrenic nucleus: a combined retrograde tracing and in situ hybridization study in the rat. Neurosci Res. 59**,** 341-6.

Yoshida, K., McCormack, S., Espana, R. A., Crocker, A., Scammell, T. E., 2006. Afferents to the orexin neurons of the rat brain. J Comp Neurol. 494**,** 845-61.

Young, A., 2005. Amylin: Physiology and Pharmacology, vol. 52. Elsevier, Academic Press, San Diego.

Zhang, Y. P., Zhu, J. N., Chen, K., Li, H. Z., Wang, J. J., 2005. Neurons in the rat lateral hypothalamic area integrate information from the gastric vagal nerves and the cerebellar interpositus nucleus. Neurosignals. 14**,** 234-43.

FIGURE LEGENDS

Fig. 1. Schematic representation of the rostro-dorsal subregion of the lateral hypothalamic area (dLHA) activated by 24 hours of fasting in rats (shaded area). The square represents the part of the dLHA displayed in Fig. 6 and 7 wherein pictures from c-Fos nuclei and BDA-labeled fiber terminals were taken. f = fornix, ic = internal capsule, opt = optic tract, ZI = zona incerta.

Fig. 2. Schematic drawings representing successful Ctb injections sites in the dLHA (A, B), brown: injections of saline-injected control animals, grey: amylin-treated animals (20μg/kg); figures adapted with permission from the Rat Brain Atlas of Paxinos and Watson (2007). Example of a successful Ctb injection into the dLHA (C) marked with an asterisk in B. Representative double stainings of Ctb labeling (brown cell bodies) and amylin-induced c-Fos expression (black-dark blue nuclei) in the AP (D), NTS (E), LPB (F), Ce (G) and BSTL (H); same animal as shown in C. High magnification picture showing the indicated LPB area (I). Arrow heads: single labeled c-Fos positive cells; thick arrow: single labeled Ctb positive neuron; thin arrows: c-Fos/Ctb double labeled neurons. Scale bars: 100 μm (C), 50 μm (D-H), 20 μm (I). scp = superior cerebellar peduncle.

Fig. 3. Quantification of c-Fos, Ctb and double positive neurons in the NTS (A), LPB (B), Ce (C) and BSTL (D) after microinjection of Ctb in the dLHA in animals injected subcutaneously with either 20 μg/kg amylin (dashed columns) or saline (black columns). Values presented as group means ± standard error; * $p<0.05$, ** $p<0.01$; *** $p<0.001$.

Fig. 4. Schematic diagrams (column A) and corresponding photomicrographs depicting the location of the amylin-activated brain areas (column B). This panel should be used as a reference for the location of BDA injection places and BDA labeled terminals shown in the following figures. Shaded areas: sites of higher (dark grey) and lower amylin-induced c-Fos expression (light grey). Arrows: c-Fos expressing areas containing black labeled nuclei. Scale bar = 100 μm. aca = anterior part anterior commisure, BSTLV = lateral division bed nucleus of the stria terminalis ventral part, BSTM = medial division BST, CC = central canal, CeC = capsular division central amygdaloid nucleus, CeL = lateral division Ce, CeM = medial division Ce, cst = commissural stria terminalis, LPBD = dorsal part lateral parabrachial nucleus, LPBI = internal part LPB, MPB = medial parabrachial nucleus, NTSDL = dorsolateral part nucleus of the solitary tract, NTSV = ventral part NTS, sol = solitary tract.

Fig. 5. Photomicrographs displaying different BDA-labeled fiber morphologies. Fibers of passage (A), terminals without (B) or with arborizations (C). Thin arrows point to varicosities and arrow heads point to arborizations. Scale bar = 20 μm.

Fig. 6. Amylin-activated areas that send projections to the fasting-activated dLHA area; top: NTS (animal #6), bottom: BSTL (animal #14). Left: BDA injection sites in the amylin-activated areas; scale bar = 100 μm. Middle and right: BDA-labeled fibers in the dLHA region within the square area represented in Fig. 1 (fiber densities indicated in upper right corners, see also Table 1); scale bar = 20 μm.

Fig. 7. LPB efferents to the fasting-activated dLHA area. Top-left: BDA injection in the LPB (animal #7). Top-right: high magnification merged photomicrographs colocalizing fasting induced c-Fos nuclei and BDA-labeled fibers in the dLHA, after BDA injection into the LPB. Arrow heads: c-Fos positive nuclei; thin arrows: fiber terminals in proximity to c-Fos-positive

nuclei. Bottom-left: fasting induced c-Fos expression in dLHA (converted photomicrographs of fluorescent staining). Bottom-right: DAB stained BDA-labeled fibers in the corresponding dLHA section (fiber density indicated in upper right corner, see also Table 1). The dLHA regions shown in the bottom images correspond to the square area shown in Fig. 1. The dashed squares within the bottom pictures show the region of the section that corresponds to the colocalization picture. Scale bar = 100 μm, except when mentioned.

Figure 1

Click here to download high resolution image

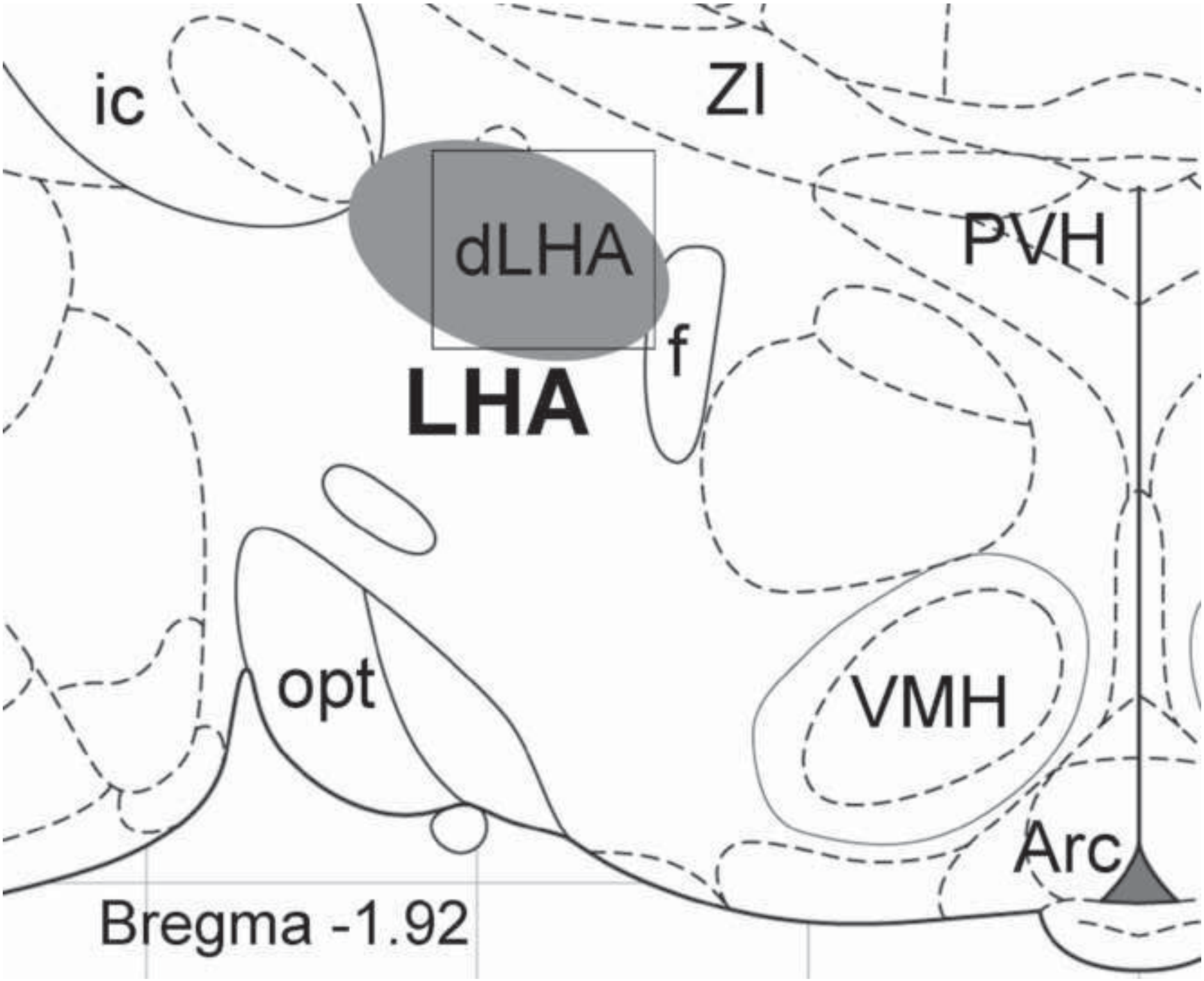

Figure 2

Click here to download high resolution image

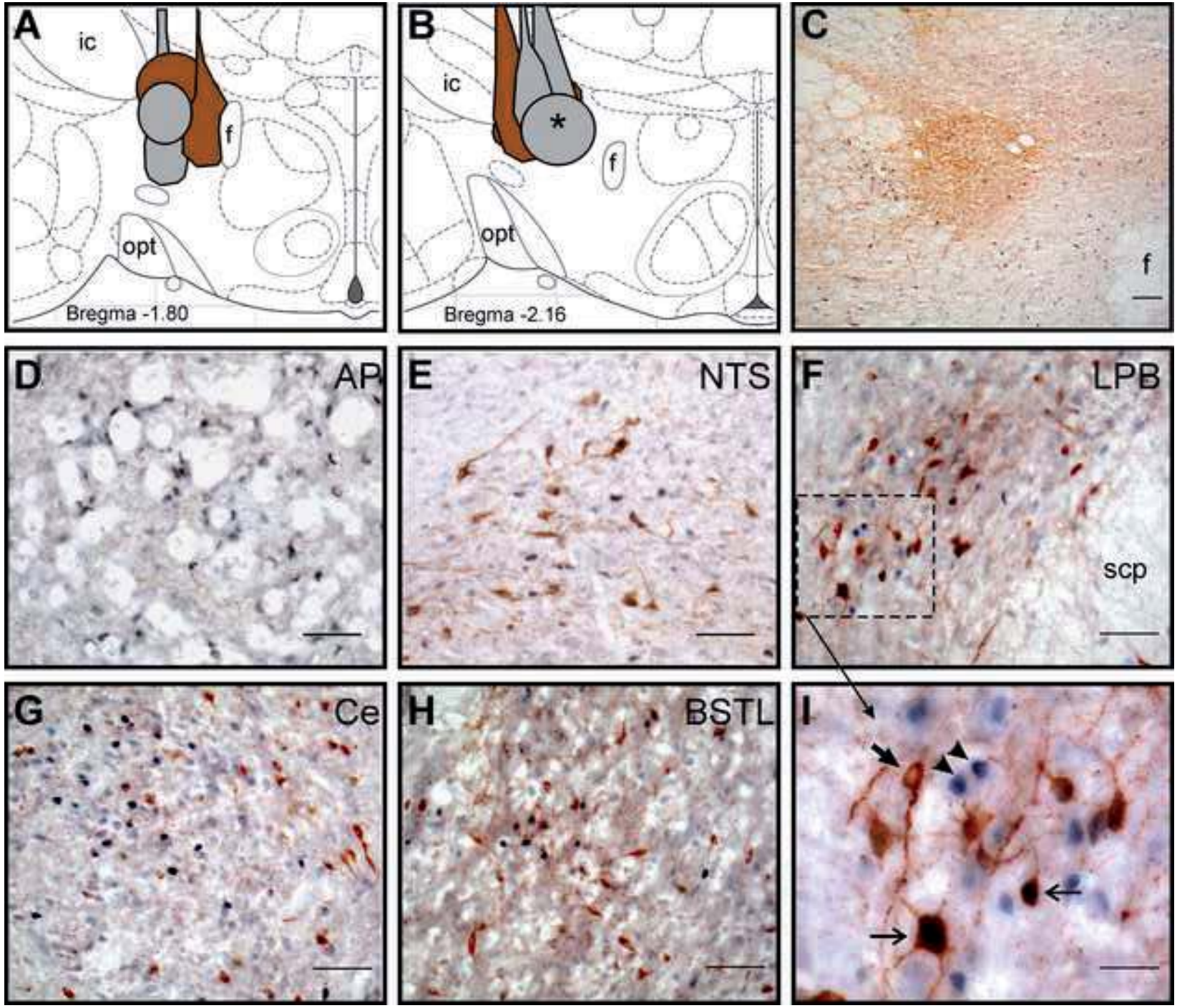

Figure 3
Click here to download high resolution image

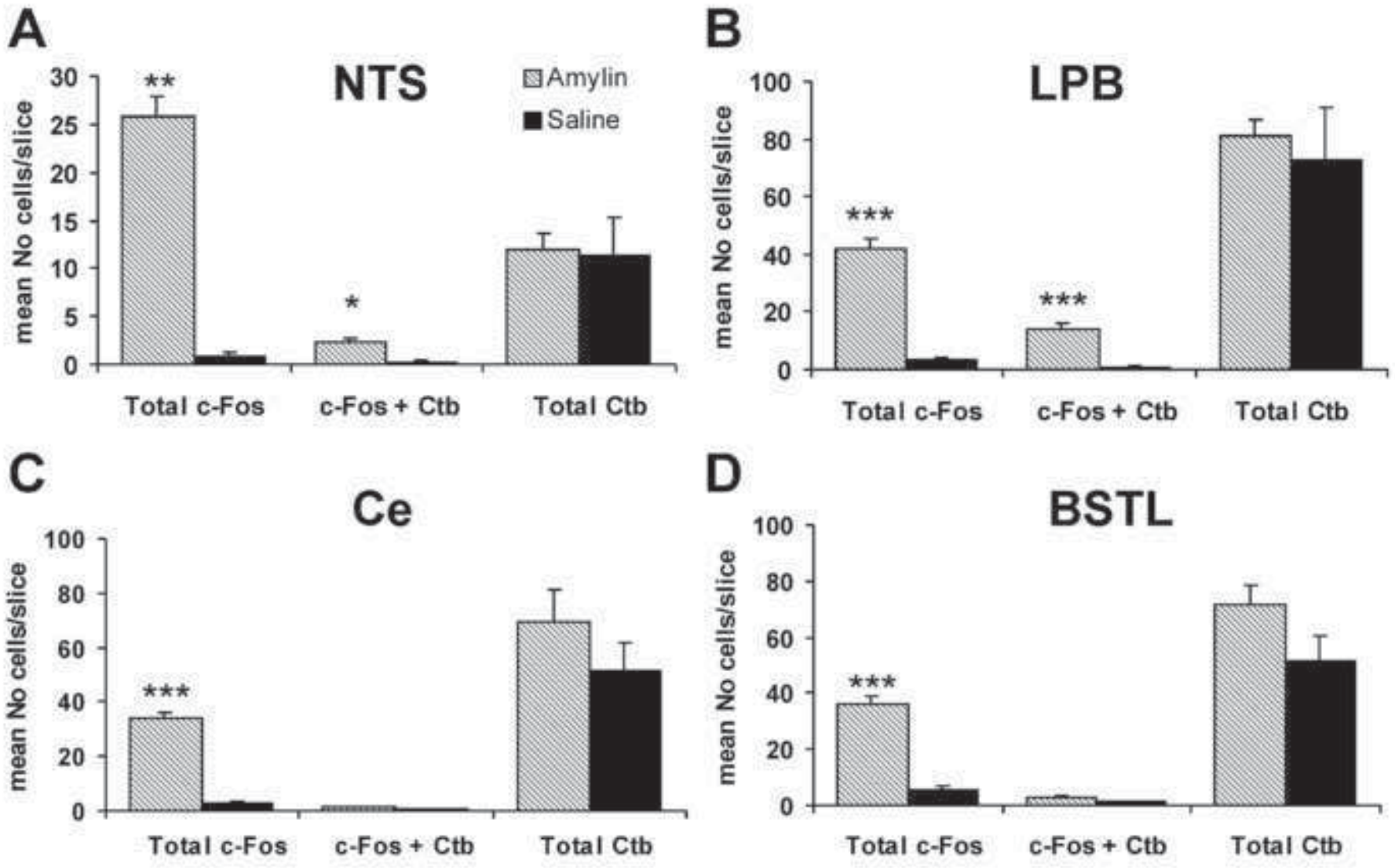

Figure 4

Click here to download high resolution image

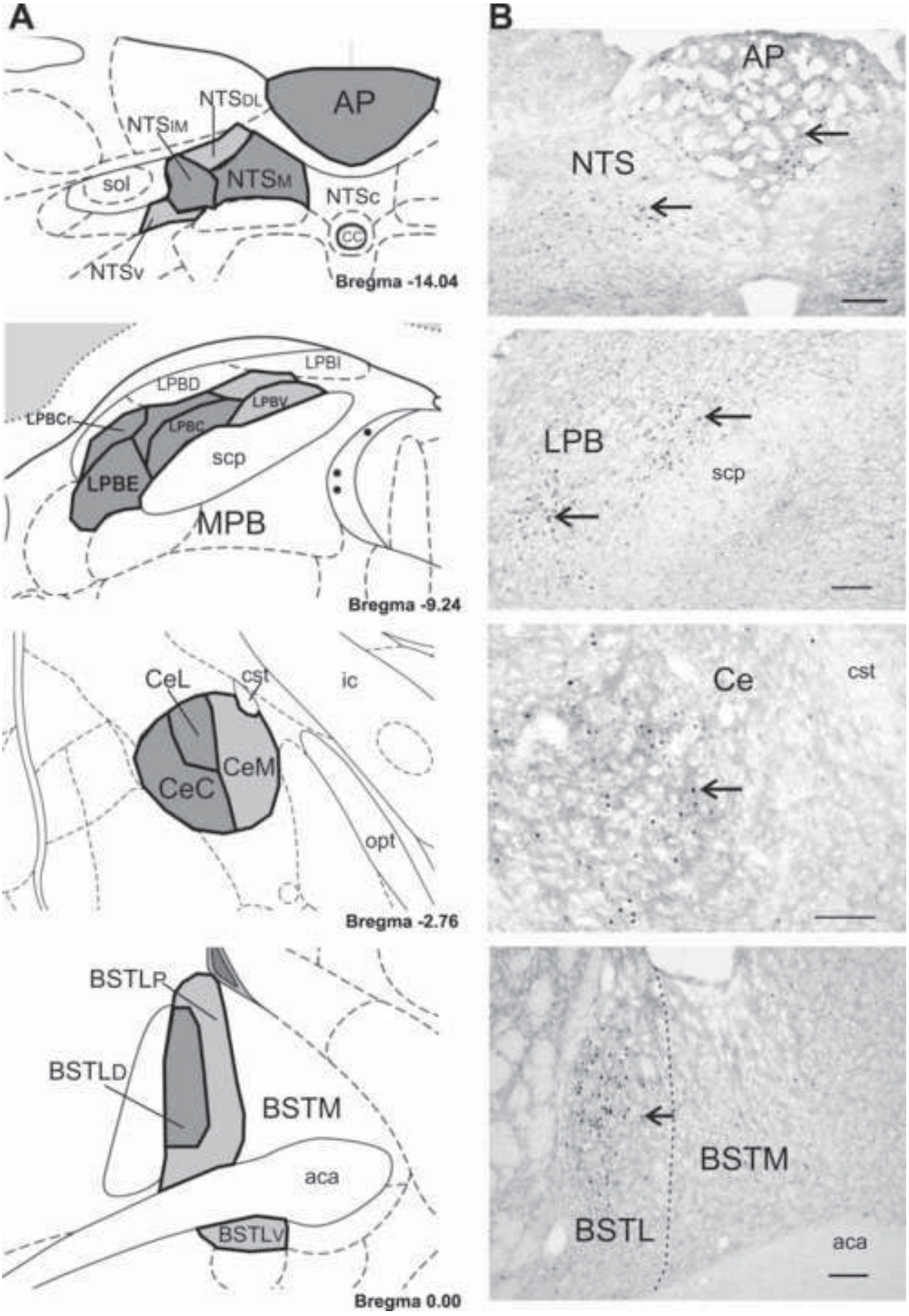

Figure 5

Click here to download high resolution image

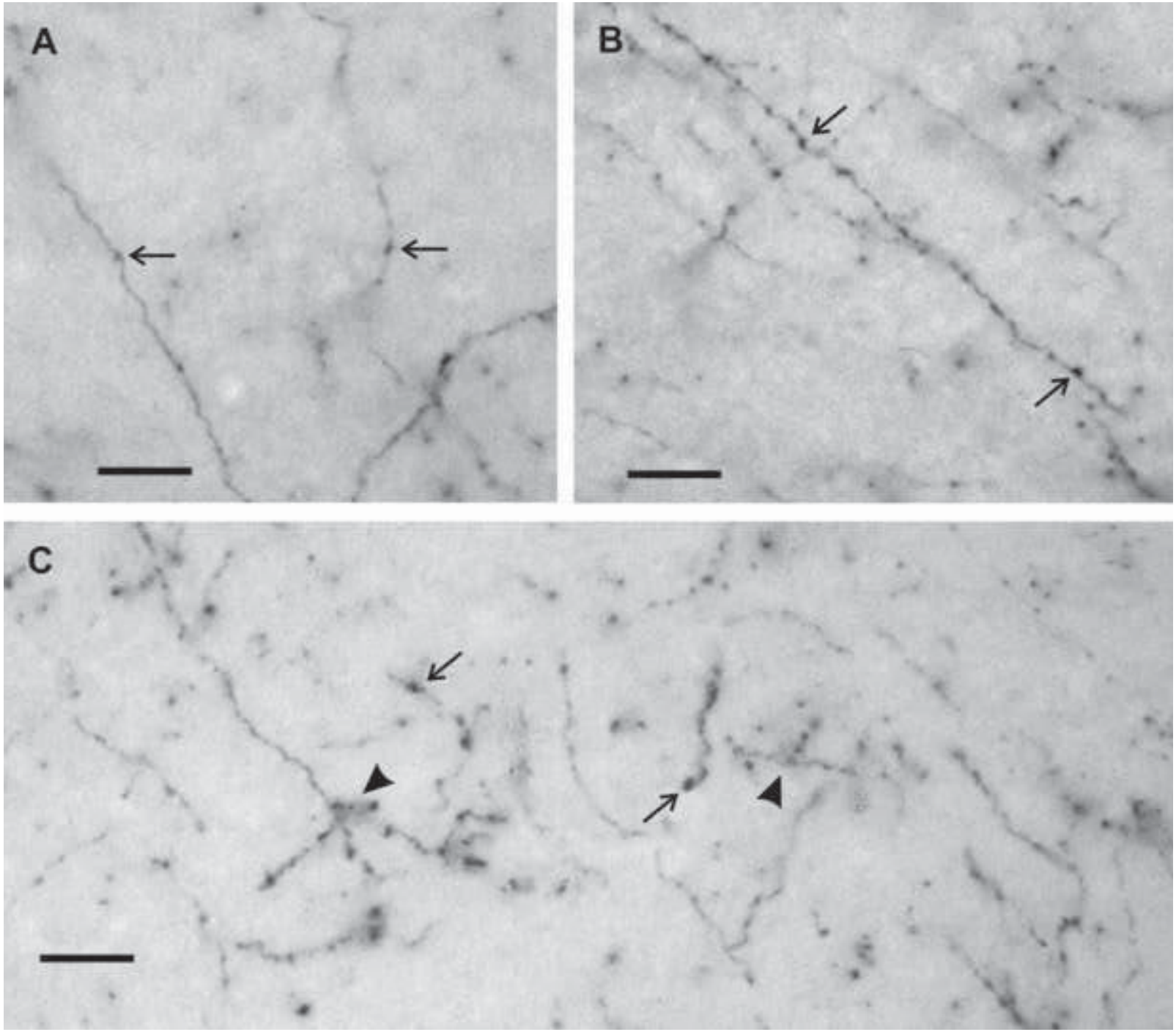

Figure 6
Click here to download high resolution image

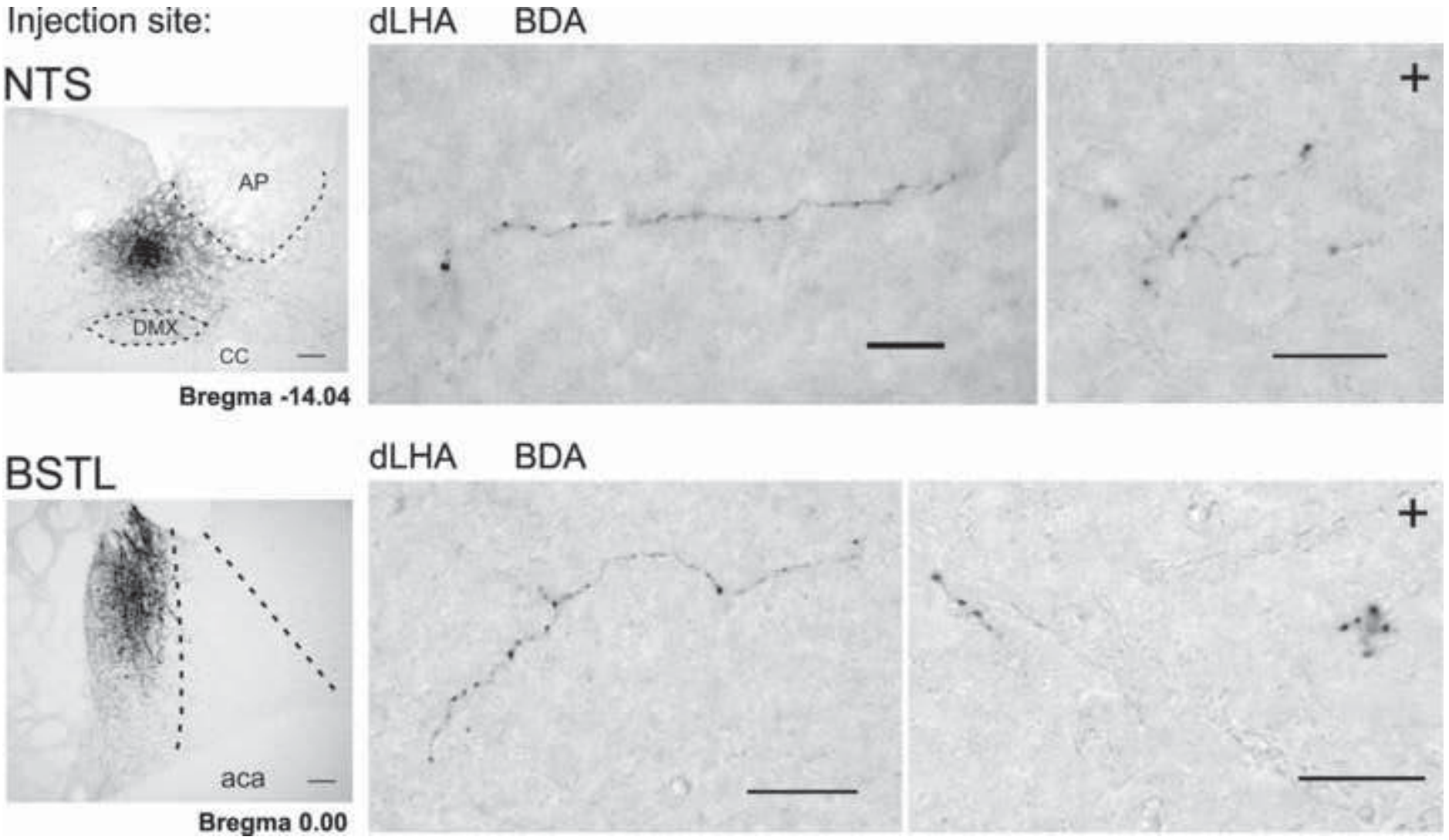

Figure 7

Click here to download high resolution image

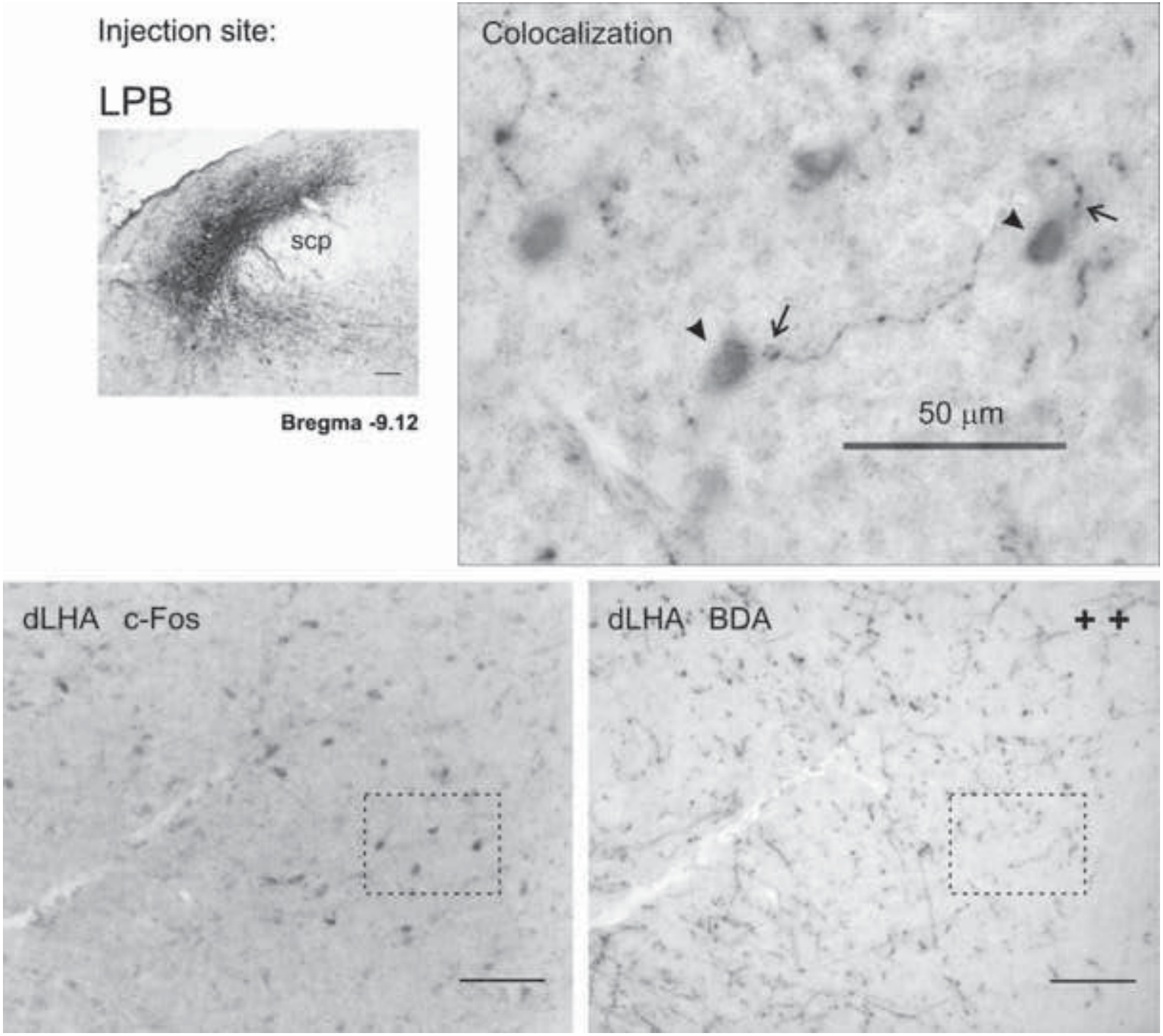

Table 1. Summary of projections observed after injections of BDA in amylin-activated areas*

Animal number	Injection place	Migration days	Relative fiber density in:									
			AP	NTS	LPB	Ce	BSTL	dLHA	Arc	VMH	DMH	PVH
1	**AP**	11	o	++	+++	-	-	-	-	-	-	-
2	**AP**	11	o	+	++	-	-	-	-	-	-	-
3	**AP**	14	o	+	++	-	-	-	-	-	-	-
4	**NTS**	10	#	o	+++	-	+	+	(+)	-	+	+
5	**NTS**	10	+	o	+++	-	+	+	(+)	-	+	+
6	**NTS**	14	+	o	+++	(+)	++	+	+	(+)	+	+
7	**LPB**	9	(+)	+	o	++++	++++	++	++	+++	++	++
8	**LPB**	9	(+)	+	o	++++	+++	++	++	++++	++	++
9	**LPB**	9	(+)	+	o	++++	++++	++	++	+++	++	++
10	**Ce**	7	-	-	++	o	+++	-	-	-	-	-
11	**Ce**	7	-	-	++	o	+++	-	-	-	-	-
12	**Ce**	14	-	++	+++	o	++++	+	-	-	+	+
13	**Ce**	14	-	++	+++	o	++++	+	-	-	+	+
14	**BSTL**	11	-	-	++	+	o	+	-	-	-	-

* Fiber density represented on a six-level scale, o injection place; - no projections; (+) very sparse; + sparse; ++ dense; +++ very dense; ++++ extensive projections; # tissue not available.